OXFORD

*Cerebral Cortex*, 2022, **32**, 3786–3798
https://doi.org/10.1093/cercor/bhab448
Advance access publication date: 17 January 2022
Original Article

# Developmental abnormalities of structural covariance networks of cortical thickness and surface area in autistic infants within the first 2 years

Ya Wang[1,2], Dan Hu[2], Zhengwang Wu[2], Li Wang[2], Wenhua Huang[1], Gang Li[2]

[1]National Key Discipline of Human Anatomy, School of Basic Medical Sciences, Southern Medical University, Guangzhou 510515, China,
[2]Department of Radiology and Biomedical Research Imaging Center, University of North Carolina at Chapel Hill, Chapel Hill, NC 27599, USA
*Address correspondence to Wenhua Huang, National Key Discipline of Human Anatomy, School of Basic Medical Sciences, 11th floor, Southern Medical University, Guangzhou 510515, China. Email: huangwenhua2009@139.com; Gang Li, The University of North Carolina at Chapel Hill, Bioinformatics Building #3104, Chapel Hill, NC 27599. Email: gang_li@med.unc.edu.

Converging evidence supports that a collection of brain regions is functionally or anatomically abnormal in autistic subjects. Structural covariance networks (SCNs) representing patterns of coordinated regional maturation are widely used to study abnormalities associated with neurodisorders. However, the possible developmental changes of SCNs in autistic individuals during the first 2 postnatal years, which features dynamic development and can potentially serve as biomarkers, remain unexplored. To fill this gap, for the first time, SCNs of cortical thickness and surface area were constructed and investigated in infants at high familial risk for autism and typically developing infants in this study. Group differences of SCNs emerge at 12 months of age in surface area. By 24 months of age, the autism group shows significantly increased integration, decreased segregation, and decreased small-worldness, compared with controls. The SCNs of surface area are deteriorated and shifted toward randomness in autistic infants. The abnormal brain regions changed during development, and the group differences of the left lateral occipital cortex become more prominent with age. These results indicate that autism has more significant influences on coordinated development of surface area than that of cortical thickness and the occipital cortex maybe an important biomarker of autism during infancy.

*Key words*: autism spectrum disorder; cortical thickness; infants; structural covariance network; surface area.

## Introduction

Autism, a complex neurodevelopmental disorder, is primarily characterized by core deficits in social interaction, repetitive or stereotypic behaviors, and sensory hypersensitivity (Association 2013). The age at diagnosis for autism is usually at 3 years and older. Currently, there are no known causes and effective cure for autism. Evidence indicates that children with autism spectrum disorders can benefit from early interventions (Landa 2018). Previous studies of infants at high familial risk for autism have provided evidence that characteristic social deficits in autism emerge in the first and second year of life and show different developmental trajectories compared with typically developing infants (Zwaigenbaum et al. 2005; Ozonoff et al. 2010; Estes et al. 2015). In addition, brain volume overgrowth was also appeared at 12 and 24 months in some infants at risk for autism who were later diagnosed with autism (Shen et al. 2013). Another research indicated that an increased rate of brain growth before age 2 years may associate with increased cortical surface area (Hazlett et al. 2011). These above observations suggest that brain developmental abnormalities in high-risk infants for autism have already occurred within 2 years of age. Therefore, the identification of early biomarkers within the first 2 postnatal years might be critical in helping improve the developmental outcomes of infants with autism.

Although neuroimaging characterizing brain development of autistic subjects prompted an increasing number of studies to understand this complex neurodevelopmental disorder, no consistent early biomarkers for autism have yet been established based on the cerebral cortical surfaces before an autism diagnosis. Due to the extremely low tissue contrast and high noise in infant brain MR images, previous studies of high-risk infants have been limited to the volume-based morphometric analyses. With the recent advance in techniques for infant brain MRI processing (Li et al. 2014; Li, Wang, et al. 2015; Wang et al. 2018; Li et al. 2019), we can now accurately reconstruct infant cortical surfaces to provide precise information of surface-related abnormal clues in early age. Thus, in this study, we intend to explore the early developmental cortical abnormalities associated with autism by virtue of the reconstructed cortical surfaces and their derived features.

Previous human neuroimaging studies consistently suggest that large-scale covariance of cortical thickness or volume exists in distributed brain regions and

**Received:** July 9, 2021. **Revised:** October 18, 2021. **Accepted:** November 1, 2021

shows systematic changes with age and disease status (Fjell et al. 2009; Alexander-Bloch, Giedd, et al.2013). Structural covariance network (SCN) analysis based on a key assumption that the covariance of regional cortical anatomy is related to synchronized maturational changes in anatomically connected neuronal populations, which may mediate through axonal connections (Alexander-Bloch, Raznahan, et al. 2013). It focuses on covarying coordinated structure of the entire brain in gray matter morphology as opposed to focus on a specific structure. Considering the neurodevelopmental conditions, the SCNs provide a valid way to investigate the developmental changes of covarying structures and it is less sensitive to noises comparing with the studies based on functional connectivity.

Autism, as a complex neurological condition, shows dysfunctional network activity rather than specific aberrant separate regions (Rudie et al. 2013). Several authors have carried out a few studies to explore the changes of brain networks in autism, including the whole brain networks and functional subnetworks such as salience network and default mode network (Zielinski et al. 2012; Rudie et al. 2013; Bernhardt et al. 2014; Zeng et al. 2017). Even though there exist inconsistent findings, autism associated specific abnormalities in brain network architecture have been observed (Bethlehem et al. 2017). In addition, many prior researches have demonstrated that autism has dynamic brain connectivity configuration within distinct age cohorts (Nomi and Uddin 2015; Long et al. 2016; Han et al. 2017). Long et al. (2016) explored the topological differences between autism and controls at different age cohorts from 6-year-olds to 18-year-olds and claimed that different information communication patterns were affected by ages. However, barely, no research focused on the developmental changes of the integration and segregation of SCNs in autistic infants within the first 2 postnatal years.

SCNs have been constructed to study the covariation patterns based on cortical thickness or gray matter volume among anatomical structures (He et al. 2007; Bassett et al. 2008). Other researchers have shown that surface area and cortical thickness, which together determine cortical volume, are confirmed to have distinct sources of genetic effects and be modulated by distinct cellular mechanisms (Panizzon et al. 2009). One radial unit hypothesis of cortical development suggests that cortical surface area is determined by the number of neuron columns that run perpendicular to the cortical surface, whereas cortical thickness is influenced by the number of cells within a column (Rakic 1988). Although other explanations such as different structural aspects might be possible, surface area is also proved following small-world properties and shows better topological organization in terms of minimal axonal length principle (Sanabria-Diaz et al. 2010). Therefore, as suitable morphometric descriptors to study the concurrent changes between brain structures, both surface area and cortical thickness were employed here to construct the group-level SCNs by correlating pairs of regions across subjects.

In this study, we detected the developmental changes of SCNs based on cortical thickness and surface area using advanced image processing techniques in autistic infants within the first 2 years after birth. The graph theoretical network analysis was employed to quantify the segregation and integration of SCNs. We chose the most classical measures, that is, clustering coefficient, local efficiency, and modularity to quantify the network segregation, which measure the strength of local connections within networks. In addition, we chose the characteristic path length and global efficiency to quantify network integration, which measure the strength of long-range connections that span discrete brain networks. Small-world property was also studied because of its ability on reflecting an optimal balance of integration and segregation (Sporns and Honey 2006). Important brain regions, which play key roles through interacting with many other regions to facilitate functional integration, were detected by regional betweenness and degree as well in our study.

## Methods

### Participants and Image Acquisition

The research data were obtained from Autism Centers of Excellence Network study funded by National Institutes of Health, referred to as the Infant Brain Imaging Study (IBIS). IBIS is an ongoing, longitudinal study of infants at a familial risk for autism. Infants were recruited, screened, and assessed at one of the four clinical data collection sites: University of North Carolina at Chapel Hill, University of Washington, Children's Hospital of Philadelphia, and Washington University in St. Louis (Hazlett et al. 2017). Data collection sites had study protocols approval from their Institutional Review Boards. Infants at high and low familial risk entered the study at 6 months of age and were followed up at 12 and 24 months of age. Informed consents provided by parents/legal guardians were obtained for all enrolled subjects. Subjects were considered as high risk if they had an older sibling with a clinical diagnosis of autism confirmed with the Autism Diagnostic Interview-Revised and subjects were collected as low risk if their older siblings have no evidence of autism and no family history of a first- or second-degree relative with autism (Hazlett et al. 2017). Exclusion criteria (Hazlett et al. 2017) include: 1) diagnosis or physical signs indicating a genetic condition or syndrome associated with ASDs; 2) significant medical or neurological condition influencing growth, development, or cognition; 3) sensory impairment, for example, vision or hearing loss; 4) prematurity (<36 gestational weeks) or low birth weight (<2000 g); 5) possible perinatal brain injury from adverse exposure (e.g., alcohol, selected prescription medications); 6) a first-degree relative having psychosis, intellectual disability, schizophrenia, or bipolar disorder; 7) non-English-speaking family; 8) contraindication for MRI (e.g., metal

**Table 1.** Basic demographical characteristics of subjects

| Characteristics | Autism ($n = 32$) | Control ($n = 41$) | $P$-values |
|---|---|---|---|
| Gender (M/F) | 24/8 | 26/15 | 0.29 |
| Age (6 months) | $6.19 \pm 0.98$ | $6.27 \pm 0.88$ | 0.72 |
| Age (12 months) | $12.25 \pm 0.66$ | $12.22 \pm 0.84$ | 0.87 |
| Age (24 months) | $24.06 \pm 0.75$ | $24.17 \pm 0.66$ | 0.52 |

implants); and 9) adoption. In this dataset, 328 infants at high familial risk were enrolled, of which 81 met the clinical DSM-IV-TR (diagnostic and statistical manual of mental disorders, edition IV, text revision) criteria (Cooper 2001) for autism at 24 months of age. Finally, 32 autistic subjects were included in this study because they have the neuroimaging data at all the three time points, that is, 6, 12, and 24 months of age. Meanwhile, 122 infants at low familial risk for autism were enrolled, of which 41 infants have the longitudinal scans at all the three time points and did not meet the criteria for autism.

The demographical information of the dataset about these two groups is summarized in Table 1. Pearson Chi-square test showed that no significant difference in gender and two sample $t$-test showed no significant difference in age between the two groups (corresponding $P$-values shown in Table 1). All images were acquired on Siemens Tim Trio 3 T scanners with 12-channel head coils, while infants were naturally sleeping and fitted with ear protection, with their heads secured in a vacuum-fixation device; 3D T1 MPRAGE MR images were acquired with 160 sagittal slices using parameters: TR/TE = 2400/3.16 ms and voxel size = $1 \times 1 \times 1$ mm$^3$; 3D T2 FSE MR images were obtained with 160 sagittal slices using parameters: TR/TE = 3200/499 ms and voxel size $1 \times 1 \times 1$ mm$^3$.

## Image Processing

Since both T1w and T2w images were available in the NDAR dataset, we used both modalities for the image processing, which provided complementary information and led to highly accurate morphological measurements of the cerebral cortex. All images were processed by iBEAT V2.0 Cloud (http://www.ibeat.cloud/), an infant dedicated pipeline (Li et al. 2014; Li, Wang, et al. 2015; Wang et al. 2018; Li et al. 2019) for tissue segmentation and cortical surface reconstruction. The major steps of the processing procedures are listed below. 1) The intensity inhomogeneities in the T1w and T2w images were corrected using the nonparametric nonuniform intensity normalization (N3) method (Sled et al. 1998). 2) The T2w images were linearly aligned onto the corresponding T1w images for each subject using FLIRT (Smith et al. 2004). 3) The skull, cerebellum, and brainstem of the aligned images were removed based on a deep learning based method (Zhang et al. 2019). 4) The brain cerebrum was labeled into white matter, gray matter, and cerebrospinal fluid (CSF) based on both the T1w and T2w images using a deep learning-based segmentation method (Wang et al. 2018). 5) The segmented cerebrum was separated into the left and right hemispheres and the noncortical regions were filled with the white matter. 6) The topological defects in each hemisphere were corrected by a learning based method (Sun et al. 2019). 7) The topology-correct and geometry-accurate inner cortical surface was first reconstructed and then further deformed to the interface of the gray matter and CSF for reconstructing the outer cortical surface (Li et al. 2014). 8) Cortical thickness and surface area were computed based on the reconstructed cortical surfaces (Fischl and Dale 2000; Li, Lin, et al. 2015). 9) The cortical parcellations were obtained by aligning the UNC 4D Infant Cortical Surface Atlas onto each individual surface (Wu et al. 2017; Wu et al. 2019) (https://www.nitrc.org/projects/infantsurfatlas/). This parcellation follows the Desikan parcellation protocol (Desikan et al. 2006) with 34 cortical regions in each hemisphere. We then constructed the structure covariance networks based on cortical thickness, surface area, and parcellations.

## Measurement of Cortical Thickness and Surface Area

Cortical thickness was measured in the native space using the shortest distance between the reconstructed inner and outer cortical surfaces at each vertex (Li et al. 2012). For each subject, regional cortical thickness was defined as the average thickness of all vertices belonging to the same region of interest (ROI). A linear regression analysis was performed at each cortical region at each age in the two groups to remove the effects of multiple confounding variables: gender, age, and whole brain overall mean cortical thickness (He et al. 2007). The residual of the regression was treated as the raw cortical thickness value of each ROI.

For each subject, regional surface area was the sum of areas of all vertices belonging to the same ROI. The confounding effects of gender, age, and total surface area were removed at each cortical region through a linear regression (He et al. 2007; Nie et al. 2013; Nie et al. 2014). The residual of the regression was treated as the raw surface area value of each ROI.

## Construction of SCNs

Through the construction of structural covariance matrices, we intended to characterize the brain networks of autism and controls. The statistical similarity between two regions was measured by computing the Pearson's correlation coefficient across subjects, and an interregional correlation matrix ($N \times N$, where $N$ is the number of brain regions, herein $N$ is 68) was constructed from each group at each age (He et al. 2007). Therefore, group level SCNs ($68 \times 68$) of cortical thickness and surface area were constructed separately for the two groups at 6, 12, and 24 months, respectively. In order to improve the normality of the correlation, correlation coefficients $r$ was then converted to z value using the Fisher transformation. By binarizing the correlation matrix using a

series of sparsity thresholds, which resulted in a certain percentages of connections, a series of unweighted and undirected graphs were obtained for subsequent network analysis. Given the fact that selection of different threshold values could cause the changes in small-world network parameters, we thresholded the correlation matrices over a wide range of sparsity (14–40%) to avoid the uncertainty resulted from the threshold choice. The chosen range of sparsity allows the small-world network architectures to be properly estimated and the number of spurious edges in each network minimized as indicated in previous studies (Achard and Bullmore 2007; He et al. 2007). All the networks in this paper demonstrated small-world architectures as they had an almost identical path length (normalized path length ≈1) but were more locally clustered (normalized clustering coefficient > 1), consistent with previous studies. The lowest threshold was identified as the minimum network sparsity in which the resultant networks were fully connected and were estimable for the small-worldness.

### Graph-Based Network Analysis

Global and regional measures of SCNs were quantified using GRETNA, a MATLAB-based toolbox for network analysis (Wang, Wang, et al. 2015) (https://www.nitrc.org/projects/gretna/). We computed normalized characteristic path length and global efficiency as the measures of network integration, and normalized clustering coefficient, local efficiency, and modularity as the measures of network segregation. The small-worldness, which reflects the optimal balance of network integration and segregation, was also computed. Nodal betweenness and degree centrality were examined to identify group differences in regional measures. The above measures of brain connectivity originally introduced by Rubinov and Sporns (Rubinov and Sporns 2010; Wang et al. 2010) are elaborated below.

The average shortest path length between all pairs of nodes in a network, known as characteristic path length, is the most commonly used measure of functional integration, which measures the extent of overall communication efficiency of a network (Watts and Strogatz 1998). Short path length ensures the efficient interactions between and across remote cortical regions, which are considered as the basis of cognitive processing (Sporns and Zwi 2004). Efficiency as a biologically relevant metric represents the capacity to exchange parallel information flow at low consumption and can be described at global and local levels (Latora and Marchiori 2001). Higher global efficiency is indicative of faster information transfer and better network integration. Clustering coefficient as the most commonly used measure of functional segregation quantifies the extent of local interconnectivity or cliquishness. High clustering coefficient ensures the functional overlap of densely connected neurons, which are functionally segregated and compose topological modules of cortical architecture (Sporns and Zwi 2004).

Measures of node centrality assess the importance of individual nodes, and the important nodes always play a key role in network resilience to insult. Betweenness is defined as the fraction of all shortest paths in the network that pass through a given node, and the nodes with high betweenness values are considered as connecting disparate parts of a network (Rubinov and Sporns 2010). The degree of a node indicates the number of edges connecting it with many other nodes in network structurally or functionally, especially in anatomical networks.

### Statistical Analysis

A nonparametric permutation test was employed to investigate the statistical differences of network metrics between two groups at three time points according to previous studies (He et al. 2008; Shi et al. 2012). First, a network measure (e.g., clustering, path length, efficiency, modularity, betweenness, and degree) was computed separately for the autism and controls. Then, we randomly reallocated each subject's set of cortical thickness or surface area values into two groups, resulting in the same sample size as the original groups. SCNs were recomputed for each of the 2 groups and new values for the network metrics were then obtained. Each permutation test was repeated 1000 times and significance was reached if less than 5% of between-group difference in the permutation distribution was greater than the observed between-group difference. Considering various densities, we compared their area under the curve (AUC) (density range of 0.14:0.02:0.4) between the two groups at each of three time points.

## Results

### The Differences of Network Segregation and Integration Measures Based on Cortical Thickness

Compared with the controls, statistical analysis indicated that the autism group showed no significant difference at the AUC of network integration, segregation, and small-worldness measures regarding cortical thickness at 6, 12, and 24 months. The developmental changes of the network integration and small-worldness at the range of sparsity (0.14–0.4) were showed in Figure 1. The variations of the network segregation were showed in Figure 2. The *P*-values for each metric were showed in Table 2.

### The Differences of Network Segregation and Integration Measures based on Surface Area

The network segregation and integration metrics of surface area showed a certain degree of difference compared with those of cortical thickness. At 6 and 12 months of age, there was no significant difference in the network measures between the two groups. At 24 months of age, the network segregation, integration, and small-worldness measures exhibit significantly different AUC between the two groups. With the increase of age, the autism group showed gradually increased

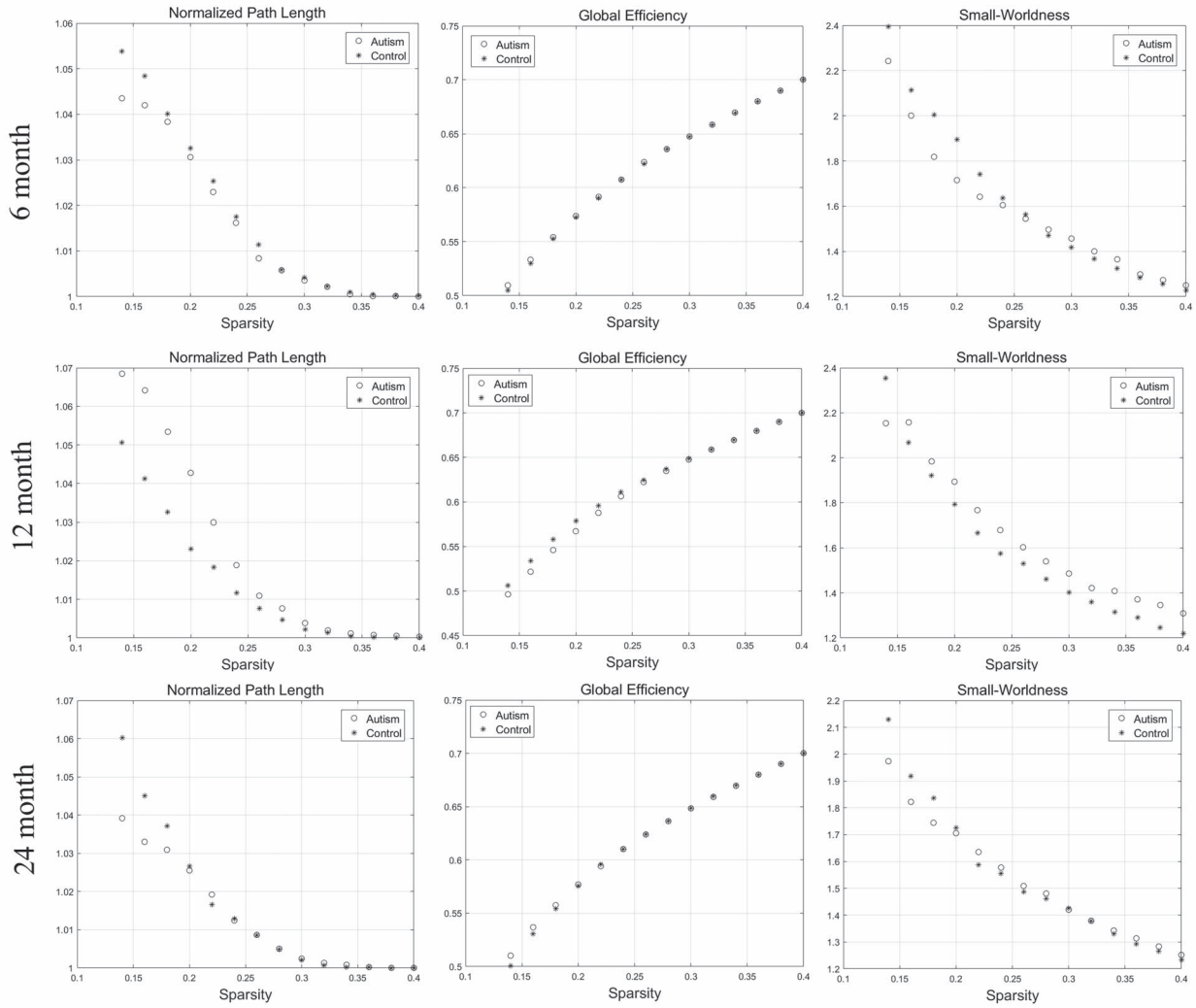


**Fig. 1.** The changes of "integration" (normalized path length and global efficiency) and "small-worldness" metrics of SCNs based on "cortical thickness" at 6, 12, and 24 months of age at the range of 14–40% network sparsity. No significant differences of AUC of the integration and small-worldness metrics between the two groups were found through statistical analysis.

integration compared with the controls, according to the decreased AUC of the characterized path length and a trend of increased global efficiency. Moreover, the small-worldness of the autism group decreased significantly at 24 months of age. The changes above were showed in Figure 3. In addition, with the increase of age, the autism group demonstrated gradually decreased segregation on account of the reduced local efficiency and clustering coefficient and a trend of decreased modularity than the controls. The changes of the segregation measures at the range of sparsity (0.14–0.4) were showed in Figure 4. The *P*-values for these metrics were listed in Table 2.

## The Differences of Network Regional Measures of Surface Area

According to permutation tests, the betweenness and degree showed significant differences between the two groups at all three time points as showed in Figure 5. At 6 months, the betweenness of the bilateral medial orbital frontal gyri, right superior parietal cortex, and right transverse temporal gyrus in the autism group significantly increased, while the betweenness of the right posterior cingulate gyrus significantly decreased. The degree of the left superior frontal gyrus, the left superior temporal gyrus, and the right caudal middle frontal gyrus in the autism group significantly decreased, while the degree of the right superior parietal gyrus and right transverse temporal gyrus significantly increased. At 12 months, the betweenness of the left banks superior temporal gyrus, left rostral middle frontal gyrus, and left temporal pole significantly decreased, while the betweenness of the left inferior temporal gyrus and right entorhinal cortex significantly increased. The degree of the left caudal middle frontal gyrus, left lateral occipital cortex, and left posterior cingulate gyrus significantly decreased, while the degree of the left parahippocampal gyrus and right paracentral gyrus significantly increased. At 24 months, the betweenness of the left lateral occipital cortex and right inferior parietal cortex significantly decreased, while the betweenness of the right medial orbital frontal gyrus and right insula significantly increased. The degree of the left lateral occipital

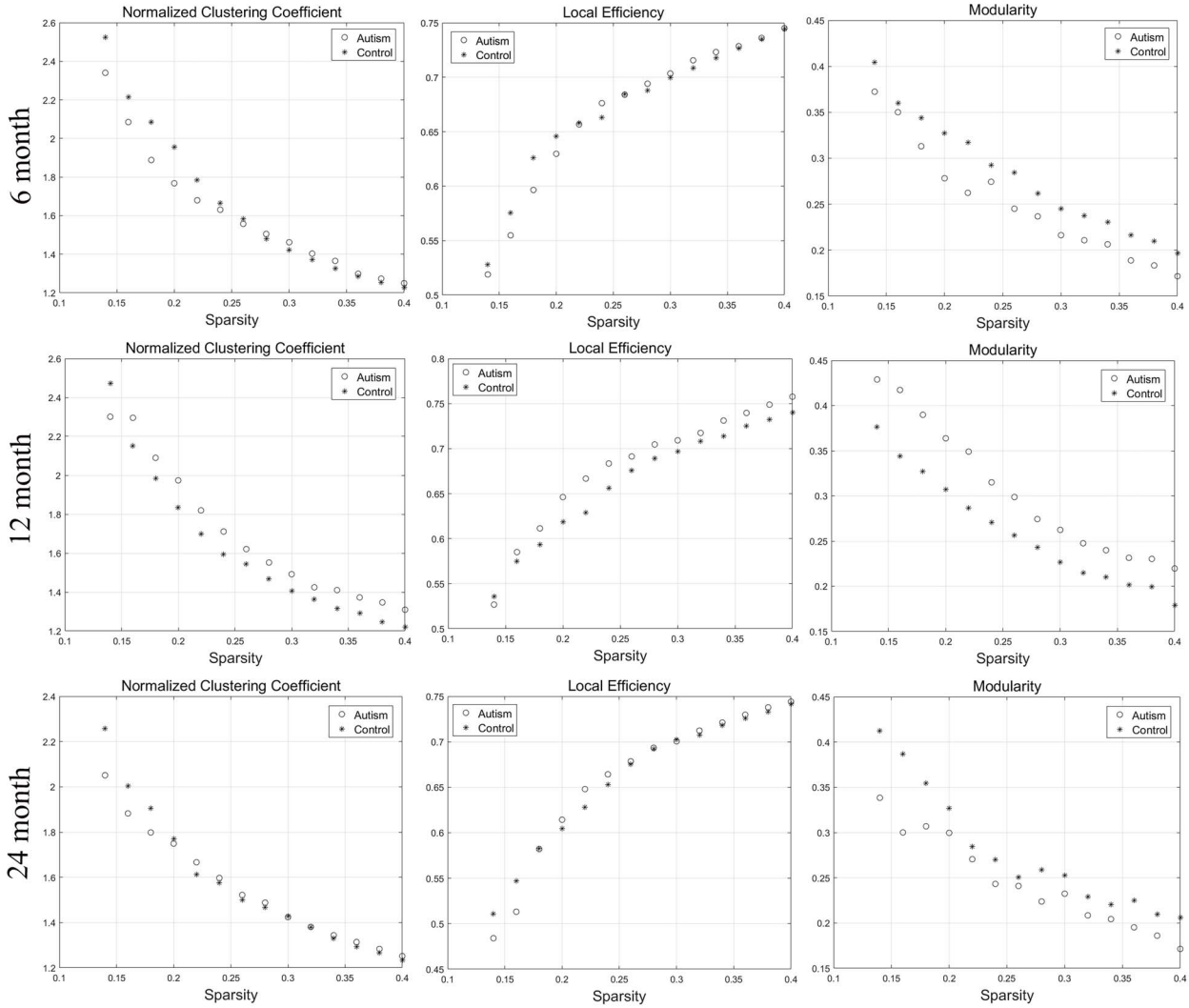


**Fig. 2.** The changes of "segregation" metrics (normalized clustering coefficient, local efficiency, and modularity) of SCNs based on "cortical thickness" at 6, 12, and 24 months of age at the range of 14–40% network sparsity. No significant differences of AUC at the segregation metrics between the two groups were found through statistical analysis.

**Table 2.** Results of permutation tests for changes in the integration and segregation measures of SCNs between the two groups across three time points within the first 2 years after birth

| P-values | Measures Age | Normalized Path Length | Global Efficiency | Small-Worldness | Normalized Clustering Coefficient | Local Efficiency | Modularity |
|---|---|---|---|---|---|---|---|
| Cortical Thickness | 6 months | 0.276 | 0.298 | 0.235 | 0.229 | 0.331 | 0.849 |
| | 12 months | 0.081 | 0.073 | 0.254 | 0.234 | 0.183 | 0.062 |
| | 24 months | 0.247 | 0.290 | 0.347 | 0.336 | 0.397 | 0.120 |
| Surface Area | 6 months | 0.367 | 0.371 | 0.432 | 0.459 | 0.384 | 0.458 |
| | 12 months | 0.297 | 0.299 | 0.221 | 0.234 | 0.197 | 0.212 |
| | 24 months | *0.039 | 0.062 | *0.004 | *0.004 | *≈0.05 | 0.055 |

*Significant difference between two groups ($P < 0.05$)

cortex, left peri calcarine cortex, and left superior parietal cortex significantly decreased, while the degree of the left middle temporal gyrus significantly increased.

## Discussion

In this article, we investigated the early developmental organizational changes of SCNs in autistic infants in the first 2 years after birth. Through the graph theoretic analysis, we showed that the developmental organizational changes of cortical thickness networks and surface area networks were very different. According to the results based on cortical thickness, we did not find any significant difference on the integration and segregation measures of SCNs at 6, 12, and 24 months of age, while the global topological properties of SCNs

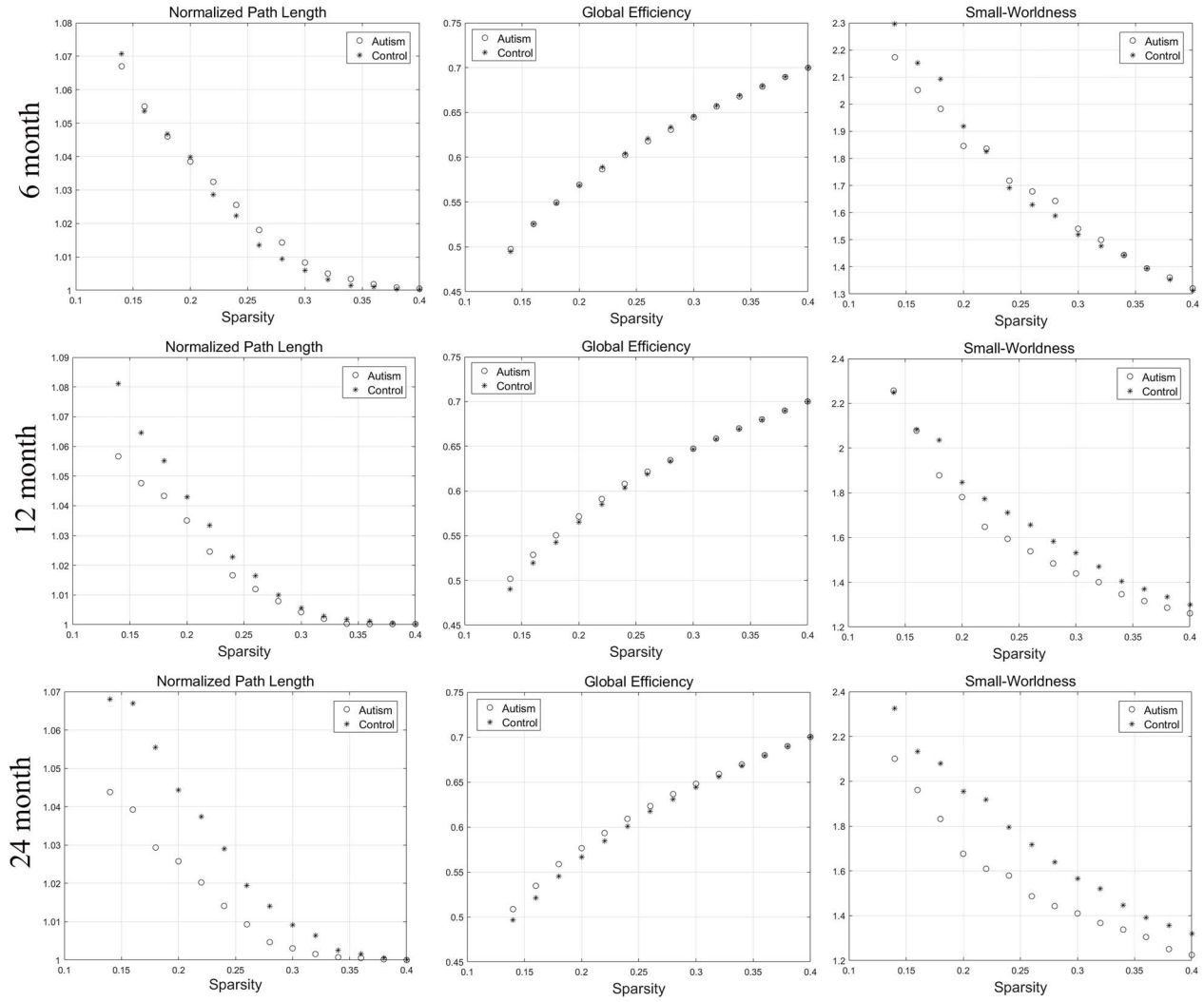


**Fig. 3.** The changes of integration (normalized path length and global efficiency) and small-worldness metrics of SCNs based on "surface area" at 6, 12, and 24 months of age at the range of 14–40% network sparsity. The autism group showed gradually decreased characterized path length, small-worldness, and increased global efficiency among the three time points. At 24 months, the characterized path length and small-worldness exhibited significant differences between the two groups through statistical analysis.

gradually changed on surface area and then showed significant differences in autistic infants at 24 months of age. The detected topological organizational changes of autistic infants revealed the increased integration and the decreased segregation, compared with the controls. In addition, the abnormal brain regions changed with age and many of them were confirmed to be related to social cognition and language processing, such as the orbitofrontal gyrus, superior parietal cortex, superior temporal gyrus, etc. The posterior regions, especially the left lateral occipital cortex in terms of surface area, may play an important role in the developmental changes of autism.

The inconsistent changes of global topological measures in the cortical thickness networks and surface area networks in autistic infants might be related to their distinct early developmental patterns and biological mechanisms. Previous studies of the developmental trajectory on cortical thickness show that the average cortical thickness increases ~40% in the first postnatal year and nearly keeps unchanged in the second year and reaches peak at ~18 months of age (Wang et al. 2019). In contrast, surface area expands ~80% during the first postnatal year and 20% during the second year and continually expands substantially thereafter (Li et al. 2013). These findings suggest that cortical thickness is relatively more established at term birth than surface area (Lyall et al. 2015), while surface area develops more rapidly during the first 2 years (Li et al. 2013). Therefore, surface area is more likely to be affected by autism mainly after birth. In addition, existing findings indicate that autism is associated with an overgrowth of cortical volume in the first 2 years of life, which are primarily caused by increased surface area rather than cortical thickness (Hazlett et al. 2011). Meanwhile, Ohta et al. (2016) illustrated that the early cortex exists overgrowth associated with autism, primarily due to the increased surface area rather than cortical thickness in 3-year-old boys. Hazlett et al. (2017)

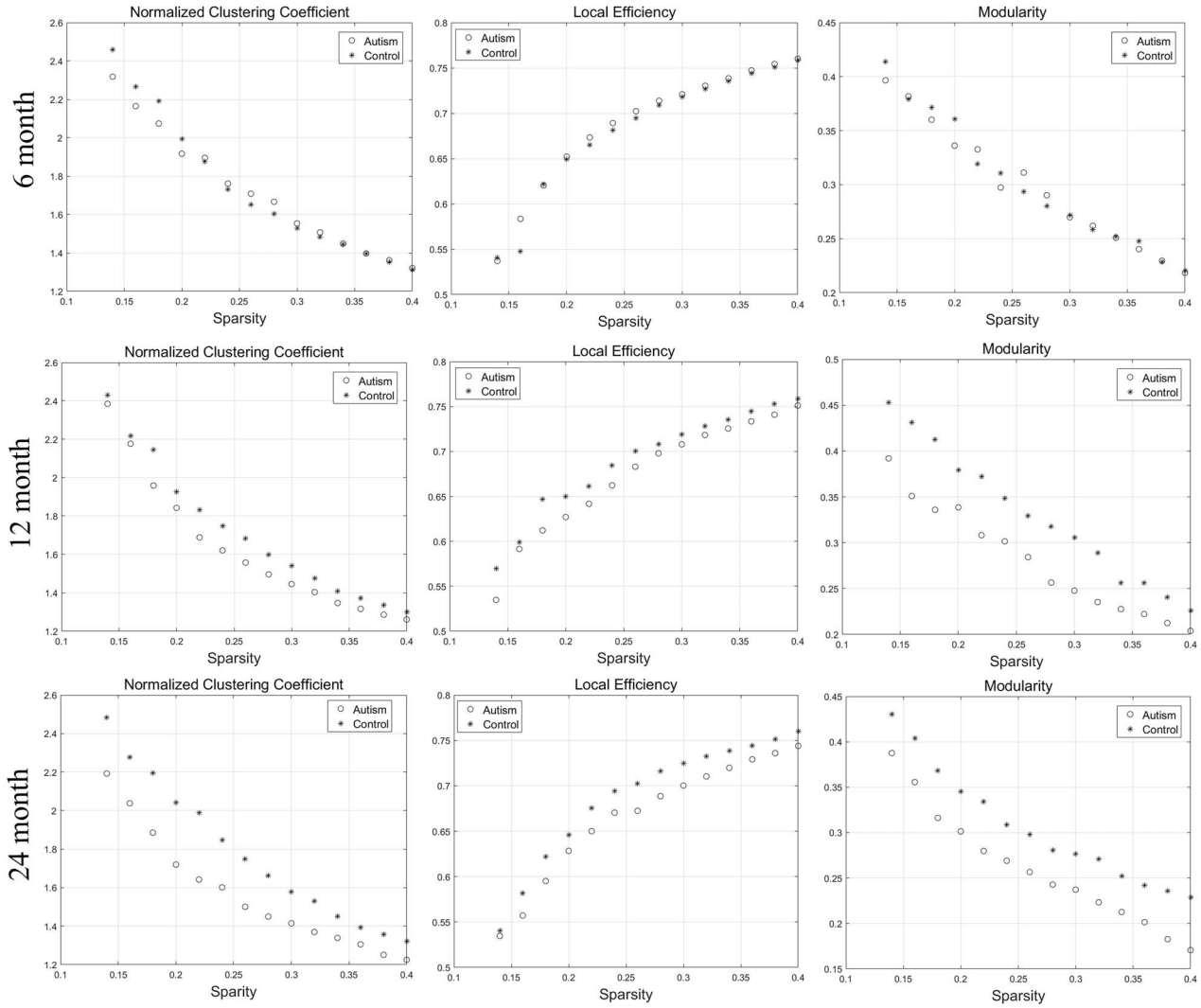


**Fig. 4.** The changes of segregation metrics (normalized clustering coefficient, local efficiency, and modularity) of SCNs based on "surface area" at 6, 12, and 24 months of age at the range of 14–40% network sparsity. The autism group showed gradually decreased clustering coefficient, local efficiency, and modularity among all the three time points. At 24 months, the clustering coefficient and local efficiency significantly decreased in the autism group compared with the control group through statistical analysis.

showed cortical surface area hyper-expansion between 6 and 12 months of age and enlargement in the total brain volume at 24 months of age and no significant difference in cortical thickness in high-risk autism group, compared with low-risk control group. In conclusion, the abnormal early cortical development in autism maybe associated with the abnormally and ununiformly increased surface area, which supports our results that the surface area network in autism infants exhibited significant changes, compared with the control group. Although no significant difference was showed in the cortical thickness networks between the two groups within the first 2 years in our study, they were observed in later childhood (Khundrakpam et al. 2017; Nunes et al. 2020). One explanation is that cortical thickness abnormalities might not emerge yet before 24 months of age, indicating the dynamic nature of morphological abnormalities in ASD. However, it is also possible that the cortical thickness difference is too subtle to be detected with the current imaging resolution (1-mm isotropic in this study). Leveraging high-resolution imaging (e.g., 0.8-mm isotropic in Baby Connectome Project or 0.5-mm isotropic in developing Human Connectome Project) and further improved surface reconstruction results might lead to new findings on cortical thickness abnormalities in autism during infancy.

Previous studies have indicated that optimized topological organization of brain anatomical networks have been established during early brain development to support rapid synchronization and information transfer and to balance between specialized processing and global integration of information (Fan et al. 2011). In this study, compared with the controls based on surface area network, we find that autism showed decreased segregation according to the decreased clustering coefficient, local efficiency, and modularity, indicating weaker regional connectivity and local information processing capacity. Based on previous studies, large-scale

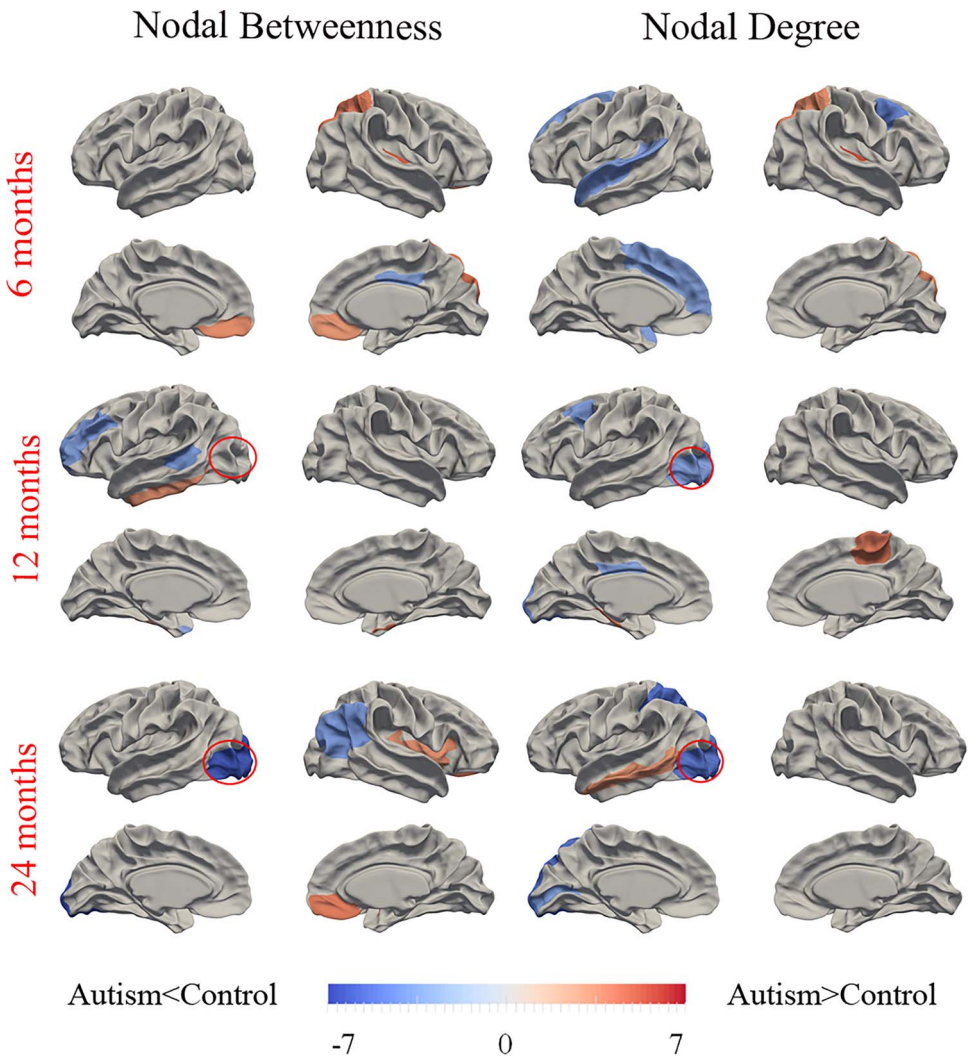


**Fig. 5.** Differences between autism and control participants in regional SCN topological metrics (betweenness and degree) at the three time points of 6, 12, and 24 months of age. Regions that showed significant differences of AUC at the range from 14% to 40% network sparsity in regional betweenness and degree between autism and controls were colored. The color bar represents log(1/*P*), where *P* is the statistical differences between the two groups. Hot/cold colors denote regions that have significantly higher/lower nodal betweenness or degree in autism than in controls, respectively. The red circles indicate the left lateral occipital cortex with changed *P*-values in nodal betweenness or degree between the two groups from 6 to 24 months of age.

disruption of inter- and intrahemispheric covariance in the left frontal SCNs for language in autism and early attentional dysfunction related to attentional networks may contribute to the weaker regional connectivity (Keehn et al. 2013; Sharda et al. 2016). The decreased path length indicates higher efficiency and less cost of message transmission along the global network of autism. The decreased segregation and increased integration reflect that the network configuration shifts toward a random network organization, which is consistent with previous results in autism based on functional brain networks (Rudie et al. 2013; Itahashi et al. 2014). Another research also showed a significant shift to randomness of brain oscillations in participants with autism by fractal analysis (Lai et al. 2010). The abnormal shift may affect the behaviors in autism through impacting the balance between local processing and global integration of information.

We employed betweenness and degree centrality the two regional network properties to identify the group differences between the autism and control infants. Nodes with high degree and betweenness suggest regions that highly interact with many other regions, facilitate functional integration, and play a key role in topological network (Rubinov and Sporns 2010). In present results, there were different sets of abnormal regions during development at 6, 12, and 24 months of age in autistic infants compared with the controls. At 6 months of age, the betweenness of the bilateral medial orbitofrontal gyri significantly increased. The functional signal of medial orbitofrontal cortex, which is involved in the cognitive process of decision-making, displayed neural hyperresponsivity to sensory stimuli and the activity was positively correlated with the level of sensory over-responsivity severity in youth with autism (Green et al. 2013). This finding is consistent with our result of

increased betweenness in this region. In addition, the betweenness and degree of the right superior parietal cortex also increased. The superior parietal cortex was confirmed to be related to visual processing and subjects with autism also showed greater functional activation in the superior parietal lobule during visual pursuit than typically developing individuals (Takarae et al. 2014), which is in line with our results. The increased interaction of the superior parietal cortex with other regions may serve as a compensatory effect in children with autism. Moreover, we did not find significant group difference in this region at 12 and 24 months of age, which may support this speculation. The left superior temporal gyrus involved in language processing and social cognition showed significant decreased degree in autism group in our results. A separate study demonstrated a reduced activation in response to auditory processing in left superior temporal gyrus in both children and adults with autism (Boddaert et al. 2004). Another study showed a failure to activate the superior temporal region in a functional MRI of voice processing in autism (Gervais et al. 2004). Taken together, the superior temporal gyrus may play a key role in language-related impairment in autism.

At 12 months of age, the betweenness of the left inferior temporal gyrus significantly increased in autism subjects. The left inferior temporal gyrus is considered to be related to transmitting large amounts of information back and forth and play a key role in learning language at early ages (Dehaene et al. 2005; Vinckier et al. 2007). A separate research confirmed increased gray matter volume in the left inferior temporal gyrus in children with autism and showed significant negative correlation between the left inferior temporal gyrus and the score of repetitive behavior in autism (Cai et al. 2018). The abnormal structure of the left inferior temporal gyrus may partially explain increased interaction with other regions in our results. In addition, the left middle frontal gyrus showed decreased betweenness and degree in our results. This region was confirmed to have decreased cerebral blood flow in childhood autism (Ohnishi et al. 2000), which was considered to be related to cognitive impairments. The functional abnormality of this region may reflect structural changes emerged in our results.

Considering the group differences of global network metrics mainly happened at 24 months, the regions with abnormal betweenness and degree centralities at 24 months may enhance the occurrence of autism. The betweenness of the right inferior parietal cortex, and the degree of the left pericalcarine and left superior parietal cortex decreased at 24 months may be disrupted with age. One previous study demonstrated that Gamma-aminobutyric acid receptors are reduced in the parietal cortex in subjects with autism, which may contribute to the disruption of the parietal cortex (Fatemi et al. 2009). Meanwhile, the nodal betweenness of the right medial orbital frontal gyrus and right insula and the degree of the left middle temporal gyrus increased at 24 months. Children with high functioning autism also showed increased functional activity in the insula, medial prefrontal cortex, and temporal cortex (Goldberg et al. 2011). These regions with increased information transfer may play an important role in maintaining or adapting to autism pathology. Considering the gradually decreased nodal betweenness and degree centralities among the three time points compared with controls, the left lateral occipital cortex may play an important role in the pathophysiology of autism. A previous study suggested that the occipital cortex showed a significantly enlarged volume in autism (Piven et al. 1996), which may serve as a compensation of abnormal local information transfer. In addition, another research also found decreased structural connectivity, resting-state brain activity, and surface area in the lateral occipital cortex in boys with autism spectrum disorder and the abnormal brain activity, and surface area in the occipital cortex was correlated with their social development (Jung et al. 2019). Therefore, the disruption of the lateral occipital cortex may be related with autism. These results were consistent with ours, which indicated that the detection of topological properties may discover some abnormal regions at the early age of autism.

Our results showed bilateral differences associated with autism. Numerous studies have confirmed language lateralization to the left hemisphere (Gaillard et al. 2003), while the behaviors caused by autism are mainly related to language processing and social cognition, which could partially explain the observed hemispheric asymmetry in autism-related abnormal regions. For example, a previous study exploring the relationships between the volume of the superior temporal gyrus and the intellectual ability confirmed no correlation in autism group, which indicated a failure in the left hemisphere lateralization of language function in autism (Bigler et al. 2007) and improved our understanding on the asymmetry of abnormal regions in autism. In addition, our relatively small sample size may influence bilateral results.

Certain limitations in this study should be noted. First, even though we revealed the regional topological alterations at three time points during infancy, we cannot verify the indicators that surely affect the autism development without behavioral measures. Further relationship between the abnormal regions and behavioral/cognitive data needs to be explored. Second, as a preliminary exploration, a larger sample size is needed to further assure the stability of our results. Third, exploration of multimodal neuroimaging, for example, diffusion and functional MR images, which can provide rich complementary information on brain connectivity, may further deepen our understanding on autism. Brain networks based on fiber connection, functional signal correlation, and structural covariance have already been employed to detect changes in topological properties in autism (Lewis et al. 2014; Kazeminejad and Sotero 2019). And researches have confirmed a tight coupling

between structural connectivity and functional connectivity, including interregional connectivity strength and network topologic organizations (Wang, Dai, et al. 2015). Combining abnormal metrics derived from different modalities may thus lead to a more comprehensive understanding of autism-related impairment during infancy.

## Conclusion

In this study, we revealed the developmental abnormalities of the topological properties in SCNs of surface area in the first 2 postnatal years of autistic infants. Decreased segregation and increased integration reflect that the network configuration shifts toward a random network organization associated with autism during infancy. The changed nodal topologies of regional surface area provide us an important reference likely related to early autism development. Taken together, the above results provide important developmental information in unraveling the biological basis of autism.

## Funding

National Institutes of Health (grants MH116225, MH123 202 to G.L., MH117943 to L.W. and G. L., MH109773 to L.W.).

## Notes

Data used in the preparation of this manuscript were obtained from the NIH-supported National Database for Autism Research (NDAR). NDAR is a collaborative informatics system created by the National Institutes of Health to provide a national resource to support and accelerate research in autism. This manuscript reflects the views of the authors and may not reflect the opinions or views of the NIH or of the Submitters submitting original data to NDAR. *Conflict of Interest*: The authors declare no conflicts of interest.

## References

Achard S, Bullmore E. 2007. Efficiency and cost of economical brain functional networks. *PLoS Comput Biol*. 3:0174–0183.

Alexander-Bloch A, Giedd JN, Bullmore E. 2013. Imaging structural co-variance between human brain regions. *Nat Rev Neurosci*. 14: 322–336.

Alexander-Bloch A, Raznahan A, Bullmore E, Giedd J. 2013. The convergence of maturational change and structural covariance in human cortical networks. *J Neurosci*. 33:2889–2899.

Association AP. 2013. Diagnostic and statistical manual of mental disorders: DSM-5. Washington (DC): American Psychiatric Association.

Bassett DS, Bullmore E, Verchinski BA, Mattay VS, Weinberger DR, Meyer-Lindenberg A. 2008. Hierarchical organization of human cortical networks in health and schizophrenia. *J Neurosci*. 28: 9239–9248.

Bernhardt BC, Valk SL, Silani G, Bird G, Frith U, Singer T. 2014. Selective disruption of sociocognitive structural brain networks in autism and alexithymia. *Cereb Cortex*. 24:3258–3267.

Bethlehem RA, Romero-Garcia R, Mak E, Bullmore E, Baron-Cohen S. 2017. Structural covariance networks in children with autism or ADHD. *Cereb Cortex*. 27:4267–4276.

Bigler ED, Mortensen S, Neeley ES, Ozonoff S, Krasny L, Johnson M, Lu J, Provencal SL, McMahon W, Lainhart JE. 2007. Superior temporal gyrus, language function, and autism. *Dev Neuropsychol*. 31:217–238.

Boddaert N, Chabane N, Belin P, Bourgeois M, Royer V, Barthelemy C, Mouren-Simeoni M-C, Philippe A, Brunelle F, Samson Y. 2004. Perception of complex sounds in autism: abnormal auditory cortical processing in children. *Am J Psychiatr*. 161:2117–2120.

Cai J, Hu X, Guo K, Yang P, Situ M, Huang Y. 2018. Increased left inferior temporal gyrus was found in both low function autism and high function autism. *Front Psychiatry*. 9:542.

Cooper J. 2001. Diagnostic and statistical manual of mental disorders (4th edn, text revision)(DSM–IV–TR). Washington, DC: American Psychiatric Association. *Br J Psychiatry*. 179:85–85.

Dehaene S, Cohen L, Sigman M, Vinckier F. 2005. Main coding schemes used in connectionist models of reading. *Trends Cogn Sci*. 7:335–341.

Desikan RS, Segonne F, Fischl B, Quinn BT, Dickerson BC, Blacker D, Buckner RL, Dale AM, Maguire RP, Hyman BT et al. 2006. An automated labeling system for subdividing the human cerebral cortex on MRI scans into gyral based regions of interest. *NeuroImage*. 31: 968–980.

Estes A, Zwaigenbaum L, Gu H, John TS, Paterson S, Elison JT, Hazlett H, Botteron K, Dager SR, Schultz RT. 2015. Behavioral, cognitive, and adaptive development in infants with autism spectrum disorder in the first 2 years of life. *J Neurodev Disord*. 7:1–10.

Fan Y, Shi F, Smith JK, Lin W, Gilmore JH, Shen D. 2011. Brain anatomical networks in early human brain development. *NeuroImage*. 54: 1862–1871.

Fatemi SH, Reutiman TJ, Folsom TD, Thuras PD. 2009. GABA a receptor downregulation in brains of subjects with autism. *J Autism Dev Disord*. 39:223–230.

Fischl B, Dale AM. 2000. Measuring the thickness of the human cerebral cortex from magnetic resonance images. *Proc Natl Acad Sci*. 97:11050–11055.

Fjell AM, Westlye LT, Amlien I, Espeseth T, Reinvang I, Raz N, Agartz I, Salat DH, Greve DN, Fischl B. 2009. High consistency of regional cortical thinning in aging across multiple samples. *Cereb Cortex*. 19:2001–2012.

Gaillard W, Balsamo LM, Ibrahim Z, Sachs BC, Xu B. 2003. fMRI identifies regional specialization of neural networks for reading in young children. *Neurology*. 60:94–100.

Gervais H, Belin P, Boddaert N, Leboyer M, Coez A, Sfaello I, Barthélémy C, Brunelle F, Samson Y, Zilbovicius M. 2004. Abnormal cortical voice processing in autism. *Nat Neurosci*. 7:801–802.

Goldberg MC, Spinelli S, Joel S, Pekar JJ, Denckla MB, Mostofsky SH. 2011. Children with high functioning autism show increased prefrontal and temporal cortex activity during error monitoring. *Dev Cogn Neurosci*. 1:47–56.

Green SA, Rudie JD, Colich NL, Wood JJ, Shirinyan D, Hernandez L, Tottenham N, Dapretto M, Bookheimer SY. 2013. Overreactive brain responses to sensory stimuli in youth with autism spectrum disorders. *J Am Acad Child Adolesc Psychiatry*. 52:1158–1172.

Han J, Zeng K, Kang J, Tong Z, Cai E, Chen H, Ding M, Gu Y, Ouyang G, Li X. 2017. Development of brain network in children with autism from early childhood to late childhood. *Neuroscience*. 367: 134–146.

Hazlett HC, Gu H, Munsell BC, Kim SH, Styner M, Wolff JJ, Elison JT, Swanson MR, Zhu H, Botteron KN et al. 2017. Early brain development in infants at high risk for autism spectrum disorder. *Nature*. 542:348–351.

Hazlett HC, Poe MD, Gerig G, Styner M, Chappell C, Smith RG, Vachet C, Piven J. 2011. Early brain overgrowth in autism associated with an increase in cortical surface area before age 2 years. *Arch Gen Psychiatry*. 68:467–476.

He Y, Chen Z, Evans A. 2008. Structural insights into aberrant topological patterns of large-scale cortical networks in Alzheimer's disease. *J Neurosci*. 28:4756–4766.

He Y, Chen ZJ, Evans AC. 2007. Small-world anatomical networks in the human brain revealed by cortical thickness from MRI. *Cereb Cortex*. 17:2407–2419.

Itahashi T, Yamada T, Watanabe H, Nakamura M, Jimbo D, Shioda S, Toriizuka K, Kato N, Hashimoto R. 2014. Altered network topologies and hub organization in adults with autism: a resting-state fMRI study. *PLoS One*. 9:e94115.

Jung M, Tu Y, Lang CA, Ortiz A, Park J, Jorgenson K, Kong X-J, Kong J. 2019. Decreased structural connectivity and resting-state brain activity in the lateral occipital cortex is associated with social communication deficits in boys with autism spectrum disorder. *NeuroImage*. 190:205–212.

Kazeminejad A, Sotero RC. 2019. Topological properties of resting-state fMRI functional networks improve machine learning-based autism classification. *Front Neurosci*. 12:1018.

Keehn B, Muller RA, Townsend J. 2013. Atypical attentional networks and the emergence of autism. *Neurosci Biobehav Rev*. 37:164–183.

Khundrakpam BS, Lewis JD, Kostopoulos P, Carbonell F, Evans AC. 2017. Cortical thickness abnormalities in autism spectrum disorders through late childhood, adolescence, and adulthood: a large-scale MRI study. *Cereb Cortex*. 27:1721–1731.

Lai MC, Lombardo MV, Chakrabarti B, Sadek SA, Pasco G, Wheelwright SJ, Bullmore ET, Baron-Cohen S, Consortium MA, Suckling J. 2010. A shift to randomness of brain oscillations in people with autism. *Biol Psychiatry*. 68:1092–1099.

Landa RJ. 2018. Efficacy of early interventions for infants and young children with, and at risk for, autism spectrum disorders. *Int Rev Psychiatry*. 30:25–39.

Latora V, Marchiori M. 2001. Efficient behavior of small-world networks. *Phys Rev Lett*. 87:198701.

Lewis JD, Evans A, Pruett J, Botteron K, Zwaigenbaum L, Estes A, Gerig G, Collins L, Kostopoulos P, McKinstry R. 2014. Network inefficiencies in autism spectrum disorder at 24 months. *Transl Psychiatry*. 4:e388–e388.

Li G, Lin W, Gilmore JH, Shen D. 2015. Spatial patterns, longitudinal development, and hemispheric asymmetries of cortical thickness in infants from birth to 2 years of age. *J Neurosci*. 35:9150–9162.

Li G, Nie J, Wang L, Shi F, Gilmore JH, Lin W, Shen D. 2014. Measuring the dynamic longitudinal cortex development in infants by reconstruction of temporally consistent cortical surfaces. *NeuroImage*. 90:266–279.

Li G, Nie J, Wang L, Shi F, Lin W, Gilmore JH, Shen D. 2013. Mapping region-specific longitudinal cortical surface expansion from birth to 2 years of age. *Cereb Cortex*. 23:2724–2733.

Li G, Nie J, Wu G, Wang Y, Shen D, Alzheimer's Disease Neuroimaging I. 2012. Consistent reconstruction of cortical surfaces from longitudinal brain MR images. *NeuroImage*. 59:3805–3820.

Li G, Wang L, Shi F, Gilmore JH, Lin W, Shen D. 2015. Construction of 4D high-definition cortical surface atlases of infants: methods and applications. *Med Image Anal*. 25:22–36.

Li G, Wang L, Yap P-T, Wang F, Wu Z, Meng Y, Dong P, Kim J, Shi F, Rekik I. 2019. Computational neuroanatomy of baby brains: a review. *NeuroImage*. 185:906–925.

Long Z, Duan X, Chen H, Zhang Y, Chen H. 2016. Structural covariance model reveals dynamic reconfiguration of triple networks in autism spectrum disorder. *SpringerOpen*. 3:1.

Lyall AE, Shi F, Geng X, Woolson S, Li G, Wang L, Hamer RM, Shen D, Gilmore JH. 2015. Dynamic development of regional cortical thickness and surface area in early childhood. *Cereb Cortex*. 25:2204–2212.

Nie J, Li G, Shen D. 2013. Development of cortical anatomical properties from early childhood to early adulthood. *NeuroImage*. 76:216–224.

Nie J, Li G, Wang L, Shi F, Lin W, Gilmore JH, Shen D. 2014. Longitudinal development of cortical thickness, folding, and fiber density networks in the first 2 years of life. *Hum Brain Mapp*. 35:3726–3737.

Nomi JS, Uddin LQ. 2015. Developmental changes in large-scale network connectivity in autism. *NeuroImage*. 7:732–741.

Nunes AS, Vakorin VA, Kozhemiako N, Peatfield N, Ribary U, Doesburg SM. 2020. Atypical age-related changes in cortical thickness in autism spectrum disorder. *Sci Rep*. 10:1–15.

Ohnishi T, Matsuda H, Hashimoto T, Kunihiro T, Nishikawa M, Uema T, Sasaki M. 2000. Abnormal regional cerebral blood flow in childhood autism. *Brain*. 123:1838–1844.

Ohta H, Nordahl CW, Iosif AM, Lee A, Rogers S, Amaral DG. 2016. Increased surface area, but not cortical thickness, in a subset of young boys with autism spectrum disorder. *Autism Res*. 9:232–248.

Ozonoff S, Iosif A-M, Baguio F, Cook IC, Hill MM, Hutman T, Rogers SJ, Rozga A, Sangha S, Sigman M. 2010. A prospective study of the emergence of early behavioral signs of autism. *J Am Acad Child Adolesc Psychiatry*. 49:256–266.

Panizzon MS, Fennema-Notestine C, Eyler LT, Jernigan TL, Prom-Wormley E, Neale M, Jacobson K, Lyons MJ, Grant MD, Franz CE. 2009. Distinct genetic influences on cortical surface area and cortical thickness. *Cereb Cortex*. 19:2728–2735.

Piven J, Arndt S, Bailey J, Andreasen N. 1996. Regional brain enlargement in autism: a magnetic resonance imaging study. *J Am Acad Child Adolesc Psychiatry*. 35:530–536.

Rakic P. 1988. Specification of cerebral cortical areas. *Science*. 241:170–176.

Rubinov M, Sporns O. 2010. Complex network measures of brain connectivity: uses and interpretations. *NeuroImage*. 52:1059–1069.

Rudie JD, Brown J, Beck-Pancer D, Hernandez L, Dennis E, Thompson P, Bookheimer S, Dapretto M. 2013. Altered functional and structural brain network organization in autism. *NeuroImage*. 2:79–94.

Sanabria-Diaz G, Melie-García L, Iturria-Medina Y, Alemán-Gómez Y, Hernández-González G, Valdés-Urrutia L, Galán L, Valdés-Sosa P. 2010. Surface area and cortical thickness descriptors reveal different attributes of the structural human brain networks. *NeuroImage*. 50:1497–1510.

Sharda M, Khundrakpam BS, Evans AC, Singh NC. 2016. Disruption of structural covariance networks for language in autism is modulated by verbal ability. *Brain Struct Funct*. 221:1017–1032.

Shen MD, Nordahl CW, Young GS, Wootton-Gorges SL, Lee A, Liston SE, Harrington KR, Ozonoff S, Amaral DG. 2013. Early brain enlargement and elevated extra-axial fluid in infants who develop autism spectrum disorder. *Brain*. 136:2825–2835.

Shi F, Yap PT, Gao W, Lin W, Gilmore JH, Shen D. 2012. Altered structural connectivity in neonates at genetic risk for schizophrenia: a combined study using morphological and white matter networks. *NeuroImage*. 62:1622–1633.

Sled JG, Zijdenbos AP, Evans AC. 1998. A nonparametric method for automatic correction of intensity nonuniformity in MRI data. *IEEE Trans Med Imaging*. 17:87–97.

Smith SM, Jenkinson M, Woolrich MW, Beckmann CF, Behrens TE, Johansen-Berg H, Bannister PR, De Luca M, Drobnjak I, Flitney DE. 2004. Advances in functional and structural MR image analysis and implementation as FSL. *NeuroImage*. 23: S208–S219.

Sporns O, Honey CJ. 2006. Small worlds inside big brains. *Proc Natl Acad Sci*. 103:19219–19220.

Sporns O, Zwi JD. 2004. The small world of the cerebral cortex. *Neuroinformatics*. 2:145–162.

Sun L, Zhang D, Lian C, Wang L, Wu Z, Shao W, Lin W, Shen D, Li G, UUBCP C. 2019. Topological correction of infant white matter surfaces using anatomically constrained convolutional neural network. *NeuroImage*. 198:114–124.

Takarae Y, Luna B, Minshew NJ, Sweeney JA. 2014. Visual motion processing and visual sensorimotor control in autism. *J Int Neuropsychol Soc*. 20:113–122.

Vinckier F, Dehaene S, Jobert A, Dubus JP, Sigman M, Cohen L. 2007. Hierarchical coding of letter strings in the ventral stream: dissecting the inner organization of the visual word-form system. *Neuron*. 55:143–156.

Wang F, Lian C, Wu Z, Zhang H, Li T, Meng Y, Wang L, Lin W, Shen D, Li G. 2019. Developmental topography of cortical thickness during infancy. *Proc Natl Acad Sci*. 116:15855–15860.

Wang J, Wang X, Xia M, Liao X, Evans A, He Y. 2015. GRETNA: a graph theoretical network analysis toolbox for imaging connectomics. *Front Hum Neurosci*. 9:386.

Wang J, Zuo X, He Y. 2010. Graph-based network analysis of resting-state functional MRI. *Front Syst Neurosci*. 4:16.

Wang L, Li G, Shi F, Cao X, Lian C, Nie D, Liu M, Zhang H, Li G, Wu Z et al. 2018. Volume-based analysis of 6-month-old infant brain MRI for autism biomarker identification and early diagnosis. *Med Image Comput Comput Assist Interv*. 2018:411–419.

Wang Z, Dai Z, Gong G, Zhou C, He Y. 2015. Understanding structural-functional relationships in the human brain: a large-scale network perspective. *Neuroscientist*. 21:290–305.

Watts DJ, Strogatz SH. 1998. Collective dynamics of 'small-world'networks. *Nature*. 393:440–442.

Wu Z, Li G, Meng Y, Wang L, Lin W, Shen D. 2017. 4D infant cortical surface atlas construction using spherical patch-based sparse representation. *Med Image Comput Comput Assist Interv*. 10433: 57–65.

Wu Z, Wang L, Lin W, Gilmore JH, Li G, Shen D. 2019. Construction of 4D infant cortical surface atlases with sharp folding patterns via spherical patch-based group-wise sparse representation. *Hum Brain Mapp*. 40:3860–3880.

Zeng K, Kang J, Ouyang G, Li J, Han J, Wang Y, Sokhadze EM, Casanova MF, Li X. 2017. Disrupted brain network in children with autism spectrum disorder. *Sci Rep*. 7:1–12.

Zhang Q, Wang L, Zong X, Lin W, Li G, Shen D. 2019. Frnet: flattened residual network for infant MRI skull stripping. In: *2019 IEEE 16th International Symposium on Biomedical Imaging*. IEEE, Italy. 2019: 999–1002.

Zielinski BA, Anderson JS, Froehlich AL, Prigge MB, Nielsen JA, Cooperrider JR, Cariello AN, Fletcher PT, Alexander AL, Lange N. 2012. scMRI reveals large-scale brain network abnormalities in autism. *PLoS One*. 7:e49172.

Zwaigenbaum L, Bryson S, Rogers T, Roberts W, Brian J, Szatmari P. 2005. Behavioral manifestations of autism in the first year of life. *Int J Dev Neurosci*. 23:143–152.